THE JOURNAL OF BIOLOGICAL CHEMISTRY VOL. 285, NO. 12, pp. 8687–8694, March 19, 2010

Mechanism for the Selective Interaction of C-terminal Eps15 Homology Domain Proteins with Specific Asn-Pro-Phe-containing Partners*

Received for publication, July 16, 2009, and in revised form, December 14, 2009 Published, JBC Papers in Press, January 27, 2010, DOI 10.1074/jbc.M109.045666

Fabien Kieken[1], **Mahak Sharma**[1], **Marko Jović**[1], **Sai Srinivas Panapakkam Giridharan, Naava Naslavsky, Steve Caplan**[2], **and Paul L. Sorgen**[3]

From the Department of Biochemistry and Molecular Biology and Eppley Cancer Center, University of Nebraska Medical Center, Omaha, Nebraska 68198-5870

Epidermal growth factor receptor tyrosine kinase substrate 15 (Eps15) homology (EH)-domain proteins can be divided into two classes: those with an N-terminal EH-domain(s), and the C-terminal Eps15 homology domain-containing proteins (EHDs). Whereas many N-terminal EH-domain proteins regulate internalization events, the best characterized C-terminal EHD, EHD1, regulates endocytic recycling. Because EH-domains interact with the tripeptide Asn-Pro-Phe (NPF), it is of critical importance to elucidate the molecular mechanisms that allow EHD1 and its paralogs to interact selectively with a subset of the hundreds of NPF-containing proteins expressed in mammalian cells. Here, we capitalize on our findings that C-terminal EH-domains possess highly positively charged interaction surfaces and that many NPF-containing proteins that interact with C-terminal (but not N-terminal) EH-domains are followed by acidic residues. Using the recently identified EHD1 interaction partner molecule interacting with CasL (MICAL)-Like 1 (MICAL-L1) as a model, we have demonstrated that only the first of its two NPF motifs is required for EHD1 binding. Because only this first NPF is followed by acidic residues, we have utilized glutathione *S*-transferase pulldowns, two-hybrid analysis, and NMR to demonstrate that the flanking acidic residues "fine tune" the binding affinity to EHD1. Indeed, our NMR solution structure of the EHD1 EH-domain in complex with the MICAL-L1 NPFEEEEED peptide indicates that the first two flanking Glu residues lie in a position favorable to form salt bridges with Lys residues within the EH-domain. Our data provide a novel explanation for the selective interaction of C-terminal EH-domains with specific NPF-containing proteins and allow for the prediction of new interaction partners with C-terminal EHDs.

The mammalian C-terminal epidermal growth factor receptor tyrosine kinase substrate 15 (Eps15)[4] homology (EH)-domain-containing (EHD) proteins are a group of four highly homologous paralogs that play distinct but overlapping roles in the regulation of endocytic transport (1). EHD proteins are composed of an N-terminal ATP-binding motif (2–4) localized between two helical regions and a C-terminal EH-domain (for review, see Ref. 1). Although there are various other proteins that contain one or more EH-domains, these proteins have their EH-domain(s) localized to the N-terminal region of the protein and fail to exhibit broad homology with the EHD family. In addition, from a functional perspective, most N-terminal EHD proteins are generally involved in the regulation of early endocytic events (such as internalization), whereas EHD proteins are more commonly implicated in controlling recycling pathways (for review, see Refs. 1, 5, 6).

EHD proteins are highly conserved in evolution, and *Caenorhabditis elegans* contain a single EHD family gene, encoding for a protein known as RME-1 that was originally identified as a critical regulator of yolk receptor recycling (7). The nearest mammalian homolog, EHD1, is involved in the regulation of endocytic recycling, primarily in controlling transport of receptors from the endocytic recycling compartment (ERC) to the plasma membrane (7–10; for review, see Ref. 1). EHD3 is the closest EHD1 paralog, displaying 86% identity, but it functions at the early endosome directing trafficking to the ERC (4) and retrograde transport to the Golgi (11). EHD1 has also been attributed a role in retrograde transport through its binding to the retromer subunit Vps35 (12). EHD4 also localizes to the early endosome and regulates trafficking to the ERC as well as to the lysosomal degradation pathway (13, 14). Several studies place EHD2 near the plasma membrane, involved in internal-

* This work was supported, in whole or in part, by National Institutes of Health Grants GM072631 (to P. L. S.), GM074876 (to S. C.), and P20RR018759 (to M. J. and N. N.). This work was also supported by the University of Nebraska Medical Center Eppley Cancer Center (P. L. S. and S. C.), Nebraska Health and Human Services Grants LB506 and 2009-38 (to P. L. S.) and LB506 and 2010-05 (to S. C.), and by an American Heart Association predoctoral fellowship (to M. S.).

The atomic coordinates and structure factors (code 2KSP) have been deposited in the Protein Data Bank, Research Collaboratory for Structural Bioinformatics, Rutgers University, New Brunswick, NJ (http://www.rcsb.org/).

[1] These authors contributed equally to this work.

[2] To whom correspondence may be addressed: Dept. of Biochemistry and Molecular Biology, 985870 Nebraska Medical Center, University of Nebraska Medical Center, Omaha, NE 68198-5870. Tel.: 402-559-7556; Fax: 402-559-6650; E-mail: scaplan@unmc.edu.

[3] To whom correspondence may be addressed: Dept. of Biochemistry and Molecular Biology, 985870 Nebraska Medical Center, University of Nebraska Medical Center, Omaha, NE 68198-5870. Tel.: 402-559-7556; Fax: 402-559-6650; E-mail: psorgen@unmc.edu.

[4] The abbreviations used are: Eps15, epidermal growth factor receptor tyrosine kinase substrate 15; EH, Eps15 homology; EHD, EH-domain-containing; ERC, endocytic recycling compartment; GST, glutathione *S*-transferase; GFP, green fluorescent protein; CHAPS, 3-[(3-cholamidopropyl)dimethylammonio]-1-propanesulfonic acid; MICAL-L1, molecule interacting with CasL-like 1; NOESY, nuclear Overhauser effect spectroscopy; HSQC, heteronuclear single quantum coherence; WT, wild-type.

ization events (15, 16), but it has also been reported to regulate ERC to plasma membrane trafficking (13).

EH-domains are well conserved structures of ~100 residues that were originally identified in three copies at the N-terminal region of Eps15 (17, 18). EH-domains contain two EF-hand helix-loop-helix motifs bridged by a short antiparallel β-sheet. Evolutionarily, although the C-terminal EH-domains of the four EHD paralogs represent a newer and more divergent subfamily, they nonetheless have three-dimensional structures that are similar to other N-terminal EH-domains (2, 19).

A major function conserved for all EH-domains studied thus far is their ability to interact with proteins that contain the tripeptide asparagine-proline-phenylalanine (NPF) (20–23; for review, see Ref. 24). The NMR solution structure of the second Eps15 EH-domain revealed that the NPF-containing peptide is found in a type I β-turn and occupies a hydrophobic binding pocket between the αB- and αC-helices on the surface of the EH-domain (20). Although there are hundreds of mammalian proteins that contain one or more NPF motifs, EHD proteins show specificity in binding to select subsets of NPF-containing proteins. Indeed, it was demonstrated that the first and third N-terminal EH-domains of Eps15R prefer binding to NPF motifs followed by an Arg residue (22).

Because the C-terminal EHD proteins carry out distinct functions from other EH-domain-containing proteins, they interact with a distinct subset of NPF-containing proteins that are involved in endocytic recycling events. Accordingly, a central question is: what regulates the selectivity of these EHDs for specific NPF-containing proteins? To address this question, we have taken advantage of two novel findings: (i) an experimental observation that despite being similar in structure to other EH-domains, C-terminal EH-domains have a highly positively charged electrostatic surface area compared with other EH-domains (19); and (ii) an empirical observation that C-terminal EH-domains appear to prefer binding to NPF motifs flanked by acidic residues (1) (see Table 1). These observations have allowed us to propose that C-terminal EH-domains do indeed prefer NPF peptides flanked by acidic residues and that the mechanism for this selectivity is derived from additional salt bridges.

EXPERIMENTAL PROCEDURES

Cloning and Purification of the EHD1 EH-domain—The human EH-domain of EHD1 (residues Asp^{436}-Glu^{534}) was subcloned into the bacterial expression vector pGEX-6P-2 (GE Healthcare) utilizing the restriction enzymes EcoRI and XhoI (PerkinElmer Life Sciences). *Escherichia coli* strain BL21 (DE-3) (Novagen) transformed with the cloned EHD1 EH-domain was grown in M63 minimum medium using 1 g of $^{15}NH_4$ and 2 g of [^{13}C]glucose (Sigma). Bacteria grown to 0.6 A_{600} were induced with 0.5 mM isopropyl 1-thio-β-D-galactopyranoside for 4 h at 37 °C and pelleted at 3,500 × *g* for 20 min. Then, the bacteria were resuspended in 1× phosphate-buffered saline containing 25× stock of Complete Protease Inhibitor (Roche Applied Science) and 1 mM dithiothreitol. The cells were lysed by a French press (three times) and pelleted by centrifugation (17,000 × *g*, 40 min) following the addition of 1 mM phenylmethylsulfonyl fluoride and 1% nonylphenoxylpolyethoxylethanol. The supernatant was bound to glutathione-Sepharose beads (Genscript) at 4 °C for 2 h. The beads were then washed with 1× phosphate-buffered saline at pH 7.4, and the EH-domain was cleaved by incubating the beads overnight at 4 °C with 80 units of PreScission Protease (GE Healthcare). The protein was separated from the beads by centrifugation (500 × *g* for 5 min) and concentrated with an Amicon ultra 10K filter (Millipore). The buffer was exchanged into 20 mM deuterated Tris, 100 mM KCl, and 2 mM $CaCl_2$ at pH 7.0 using the desalting column Econo Pac 10DG (Bio-Rad). The purity of the protein was confirmed by electrophoresis gel and the concentration determined by UV reading at 280 nm.

GST Pulldown—For GST pulldown experiments, HeLa cells were transfected with constructs containing GFP-tagged full-length molecule interacting with CasL (MICAL)-Like 1 (MICAL-L1) constructs or mutants (as indicated), harvested, and lysed for 15 min in buffer containing 25 mM Tris-HCl, pH 7.4, 125 mM NaCl, 1 mM $MgCl_2$, 0.5% CHAPS, and protease inhibitors (Sigma). After removal of insoluble matter by centrifugation, the lysate supernatants were incubated with GST-EH-1 bound to goat anti-GST antibody (Amersham Biosciences)-bound protein G beads for 2 h. The beads were then washed with phosphate-buffered saline. Proteins were separated by 8% SDS-PAGE, blocked in 5% nonfat milk in phosphate-buffered saline, and immunoblotted with mouse anti-GFP antibodies (Roche Applied Science), and detected using goat anti-mouse horseradish peroxidase. Enhanced chemiluminescence was used for detection.

NMR and Molecular Modeling—NMR data were acquired at 25 °C using Varian INOVA 600 and 800 spectrometers fitted with a cold probe at the University of Nebraska Medical Center NMR Facility and the National Magnetic Resonance Facility at Madison. The MICAL-L1 peptide NPFEEEEED was purchased from Anaspec (Fremont, CA). Backbone assignments of the EHD1 EH-domain in complex with the MICAL-L1 peptide were confirmed using HNCACB spectra. Peptide assignment was achieved using F1,F2-^{13}C,^{15}N-filtered NOESY (mixing time of 150 and 300 ms). Distance constraints were derived from ^{15}N-NOESY-HSQC, ^{13}C-NOESY-HSQC (aliphatic and aromatic), F1,F2-^{13}C,^{15}N-filtered NOESY, ^{13}C-edited-^{13}C or ^{15}N-filtered NOESY, and F2-^{13}C,^{15}N-filtered NOESY experiments (mixing time of 150 ms). Molecular modeling using ARIA 1.2 (26) and evaluation of the lowest energy structures using PROCHECK-NMR (27) were performed as described previously (19). The coordinates of the EHD1 EH-domain in the presence of the MICAL-L1 peptide have been deposited in the Protein Data Bank (2KSP) and visualized using MOLMOL software (28). The chemical shift assignments and NMR restraints used during the molecular modeling were deposited in the BioMagResBank (16671).

Binding isotherms were obtained from gradient-enhanced two-dimensional ^{1}H,^{15}N-HSQC experiments. Data were acquired with 1,024 complex points in the direct dimension and 64 in the indirect dimension. Sweep widths were 8,000 Hz in the proton dimension and 2,100 Hz in the nitrogen dimension. Dissociation constants (K_D) were calculated by nonlinear best fitting the H-N titration curves using GraphPad Prism 5.0 (GraphPad Software, La Jolla, CA), averaging over the five

TABLE 1

Comparison of the residues flanking NPF motifs from known and potential EHD interacting proteins

Known human EHD interaction partners with acidic residues flanking the NPF motif	
Rabenosyn-5 NPF1	NPFDEEDLSSPMEE
Rabenosyn-5 NPF2	NPFEEEDEEEEAVA
Rab11-FIP2 NPF1	NPFEESSETWDSS-
Rab11-FIP2 NPF3	NPFDATAGYRSLTY
SyndapinII NPF1	NPFEDEDDTGSTVS
SyndapinI NPF2	NPFEDDSKGVRVRA
SyndapinII NPF3	NPFDDDATSGTEVR
SNAP29 NPF	NPFDDDGEDEGARP
EHBP1 NPF1	NPFDDPDAAELNPF
EHBP1 NPF4	NPFDEPEAFVTIKD
Partial list of potential human EHD interaction partners with acidic residues flanking the NPF motif	
EXOC84	NPFEDDEEEEPAVP
MKRN4	NPFDDEEEAVTFEL
AAK1	NPFDDDNFSKLTAE
LYST	NPFEETADGDVYYP
TTC3	NPFEERQGEISRIE
ANFY1	NPFEDVPVVNGTSF
COR2A	NPFDDFEIASCSED
SDC10	NPFDDIIPREIKRL
SG269	NPFDENPELKEREY
Partial list of human proteins containing NPF motifs flanked by arginine	
SYNJ1	NPFRAKSEESEATS
TBD2A	NPFRMKQLRQLRMV
PKHA5	NPFRTTQTRRRDDK
PA2G6	NPFRVKEVAVADYT
IRS4	NPFRSSPLGQNDNS
ALK	NPFRVALEYISSGN
STAR9	NPFRSREGVRESEP
ZMY15	NPFRSPFRLRAADN
ZYX	NPFRPGDSEPPPAP

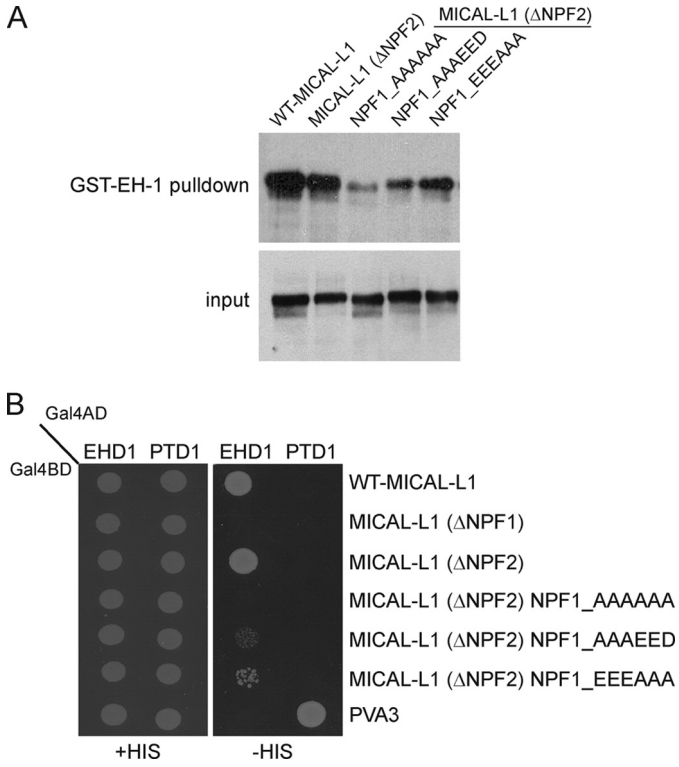

FIGURE 1. **Characterizing the interaction between the EHD1 EH-domain and MICAL-L1.** *A*, HeLa cells were transfected with GFP-tagged versions of either wild-type MICAL-L1 (*WT-MICAL-L1*), MICAL-L1 with the second NPF motif changed to APA (*MICAL-L1 (ΔNPF2)*), MICAL-L1 with the second NPF motif changed to APA and AAAAAA flanking the first NPF (*MICAL_L1 (ΔNPF2) NPF_AAAAAA*), MICAL-L1 with the second NPF motif changed to APA and AAAEED flanking the first NPF (*MICAL_L1 (ΔNPF2) NPF_AAAEED*), or MICAL-L1 with the second NPF motif changed to APA and EEEAAA flanking the first NPF (*MICAL_L1 (ΔNPF2) NPF_EEEAAA*). Purified GST-EH-1 was used to pull down wild-type and mutant GFP-MICAL-L1 from the lysates (*top panel*, immunoblot with anti-GFP). 5.5% of the total lysates were immunoblotted to show overall expression levels of the transfected proteins (5.5% input; *bottom panel*). *B*, *S. cerevisae* yeast strain AH109 was co-transformed with Gal4AD and Gal4BD fusion constructs containing either EHD1 or different MICAL-L1 constructs (*labeled* in the *panel*). Co-transformants were assayed for their growth on nonselective (+*HIS*) and selective (−*HIS*) medium. PTD1 and PVA3 served as a positive control for protein-protein interactions.

curves. Chemical shift variation was calculated according to the formula $\Delta\sigma = \sqrt{((\Delta\delta_{HN})^2 + (\Delta\delta_{N/5}))^2}$. The concentration of EH-domain was maintained constant at 50 μM.

Yeast Two-hybrid Analysis—The yeast-two-hybrid assay was done as described previously (29). Briefly, the *Saccharomyces cerevisiae* strain AH109 (BD Biosciences Clontech) was maintained on YPD agar plates. Transformation was done by the lithium acetate procedure as described in the instructions for the MATCHMAKER two-hybrid kit (BD Biosciences Clontech). For colony growth assays, AH109 co-transformants were streaked on plates lacking Leu and Trp and allowed to grow at 30 °C, usually for 3 days, or until colonies were large enough for further assays. An average of three to four colonies was then chosen and suspended in water, equilibrated to the same *A*600 nm, and replated on plates lacking leucine and Trp (+His) as well as plates also lacking histidine (−His). In addition to regular −His plates, some replatings were also done on −His plates containing 2 and 10 mM 3-amino-1,2,4-triazole (Fluka, Buchs) to validate further specificity of the interactions.

RESULTS

Acidic Residues Flanking NPF Motifs Fine Tune the Affinity of Binding to C-terminal EH-domains—Previously, we identified a cluster of positively charged surface residues within the EH-domain binding pocket and proposed that C-terminal EH-domains may potentially have a higher affinity for proteins containing the negatively charged peptide Asp-Pro-Phe (DPF) rather than NPF. Subsequent experimentation by surface plasmon resonance proved that this hypothesis was incorrect and that C-terminal EH-domains bind NPF-containing peptides with an affinity of 10-fold higher than DPF-containing peptides (30). Accordingly, our observation that the NPF-containing proteins that interact with EHDs generally have acidic clusters flanking the NPF motif (Table 1) has allowed us to revise our hypothesis, and we now propose that C-terminal EH-domains utilize an evolutionarily divergent positively charged surface area to bind a subset of NPF-containing proteins selectively: those that contain acidic residues following the NPF tripeptide.

To analyze the impact of having acidic residues following the NPF motif in the binding of NPF-containing proteins with C-terminal EH-domains, we took advantage of our recent discovery that EHD1 binds to MICAL-L1 (31), which is a member of the molecule interacting with CasL family of proteins (32). MICAL-L1 contains two NPF motifs, with the first one followed by a cluster of acidic residues (NPFEEEEED), whereas the second one had no flanking acidic residues. As demonstrated in Fig. 1, upon pulldown and two-hybrid experiments with GST-tagged full-length EHD1 or the EHD1 EH-domain (EH-1) alone, both wild-type MICAL-L1 and MICAL-L1 with a mutated second NPF motif to APA displayed similar levels of

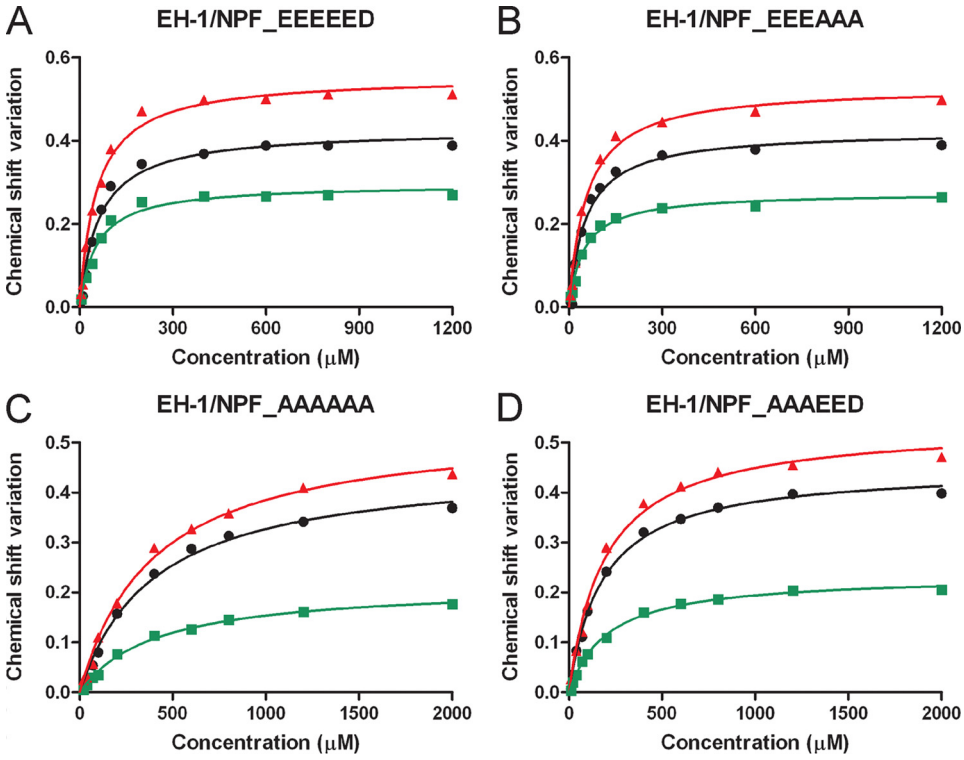

FIGURE 2. **Binding analysis of the interaction between the EHD1 EH-domain and MICAL-L1.** ^{15}N-HSQC of the EH-domain with different concentrations of MICAL-L1 wild type peptide NPF_EEEEED (*A*) and the Glu-to-Ala substituted peptides NPF_EEEAAA (*B*), NPF_AAAAAA (*C*), and NPF_AAAEED (*D*) is shown. The same three EH-domain residues (Val^{472}, *red*; Gly^{482}, *black*; and Trp^{485}, *green*) were evaluated for each peptide. Each K_D was estimated by nonlinear best fitting the chemical shift variation (in parts/million) *versus* the concentration of peptide.

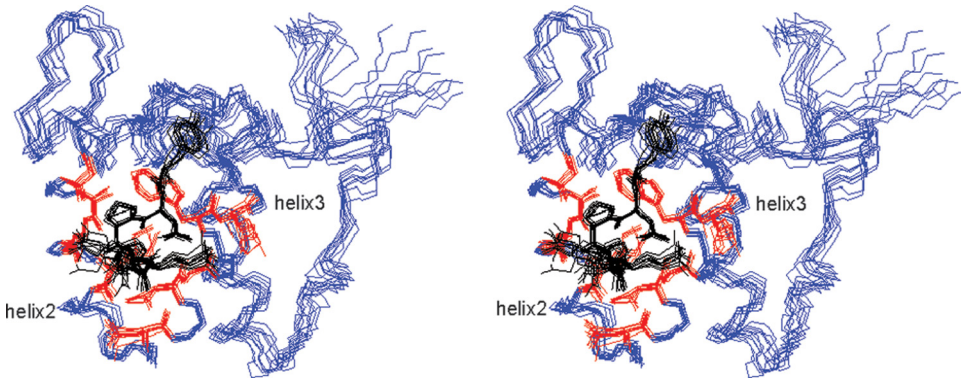

FIGURE 3. **Stereoview of the 10 lowest energy structures of the EHD-1 EH-domain in complex with the wild-type MICAL-L1 NPF_EEEEED peptide.** The structures of the EH-domain in complex with the wild-type MICAL-L1 peptide have been superimposed according to the backbone atoms of the following residues: EHD1, Gly^{464}, Ala^{467}, Lys^{468}, Met^{471}, Asn^{478} Leu^{481}, Gly^{481}, Trp^{485}, Lys^{486}; and MICAL-L1 peptide, Tyr, Asn, Pro, Phe, Glu1, and Glu2 (EH-domain, *blue*; peptide, *black*). The lateral chains of these EH-domain residues have been labeled (*red*).

binding to EH-1 (Fig. 1). However, upon mutation of the first NPF (containing the acidic cluster) to APA, the binding of MICAL-L1 to EH-1 was entirely abrogated (Fig. 1*B*). To analyze the significance of the flanking acidic residues, we utilized a simplified system with the MICAL-L1 protein containing only the first, acidic-flanked NPF motif intact. In this background, we first substituted the acidic cluster for 6 Ala residues (NPFEEEEED to NPFAAAAAA). As shown (Fig. 1), the binding to EH-1 was almost entirely lost. To delineate which of the acidic residues are most important for potentiating the binding, we then substituted either the first three Glu for Ala (NPFEEEEED to NPFAAAEED), or we substituted the next three acidic residues for Ala (NPFEEEEED to NPFEEEAAA). Although NPFEEEAAA still displayed considerable binding to EH-1, there was significantly reduced binding of the MICAL-L1 containing NPFAAAEED. These data strongly suggest that the proximal acidic residues flanking the NPF motif are required for optimal binding to C-terminal EH-domains.

The observation that the first three Glu are important for optimal binding to the EH-1 was measured quantitatively by NMR (Fig. 2). The dissociation constant (K_D) was calculated for the EH-1 interaction with wild-type MICAL-L1 peptide NPFEEEEED and the Glu-to-Ala substituted peptides NPFAAAAAA, NPFEEEAAA, and NPFAAAEED. The binding affinity for the wild-type MICAL-L1 peptide (57 μM ± 6) was significantly higher than that of the NPFAAAAAA (399 μM ± 6) and NPFAAAEED (193 μM ± 13) peptides; however, the NPFEEEAAA peptide retained an affinity that was similar to that of the wild-type MICAL-L1 peptide (54 μM ± 5). The data suggest that although the NPF motif is critical for binding EH-1, the first three Glu are necessary for a higher affinity interaction, with the last three acidic residues (EED) playing only a minor role in the association.

Structure of the C-terminal EHD1 EH-domain with the Wild-type MICAL-L1 Peptide—The structure of the complex was solved with the EH-domain (600 μM) in presence of 2 mM wild-type MICAL-L1 peptide. The backbone view of the final 10 structures of the EH-domain-wild-type MICAL-L1 peptide complex is displayed in Fig. 3, and structural information is presented in Table 2. The EH-domain in complex with the wild-type MICAL-L1 peptide NPFEEEEED shows the same general organization as the unbound domain with two associated helix-loop-helix motifs with the loops connected by a short antiparallel β-sheet. The NPF motif presents a classic type I β-turn for NPF motif binding EH domains; stabilized by hydrogen bonds between the carbonyl oxygen and the acyl oxygen of Asn with the amide protons of the Thr and Phe, respectively. Lys^{468}, Met^{471}, Val^{472}, Asn^{478}, Leu^{481}, and Trp^{485} formed a pocket where the Phe is buried between

TABLE 2

Structural statistics of the 10 lowest energy structures of the EHD1 EH-domain in complex with the wild-type MICAL-L1 peptide

Conformational Restraints		
NOE distance restraints		
Total		2786
Intra-residue (|i-j|=0)		1123
Sequential (|i-j|=1)		607
Medium range (2≤|i-j|<5)		416
Long range (|i-j|≥5)		555
Intermolecular		85
Backbone hydrogen bonds		70
Residual Violations		Average Number per residue
Distance restraints > 0.3 Å		1
Distance restraints > 0.5 Å		0
RMSD[a] from Standard Geometry		
Bond lengths (Å)		0.0035 ± 0.0002
Bond angles (degrees)		0.53 ± 0.02
Impropers (degrees)		1.39 ± 0.07
Energies		
NOE		37 kcal/mol ± 6
Van der Waals		-1060 kcal/mol ± 17
Electrostatic		-5633 kcal/mol ± 68
Ramachandran Maps		
Residues in most favored regions		83.3%
Residues in additional allowed regions		15.5%
Average RMSD[a]	Backbone (Å)	All non-hydrogens (Å)
EH-domain$_{W439-S529}$	0.73 ± 0.10	1.19 ± 0.09
EH-domain$_{W439-S529}$/MICAL-L1$_{Y-E3}$	0.73 ± 0.09	1.18 ± 0.09
MICAL-L1$_{Y-E3}$	0.35 ± 0.15	0.70 ± 0.14

[a] RMSD, root mean square deviation.

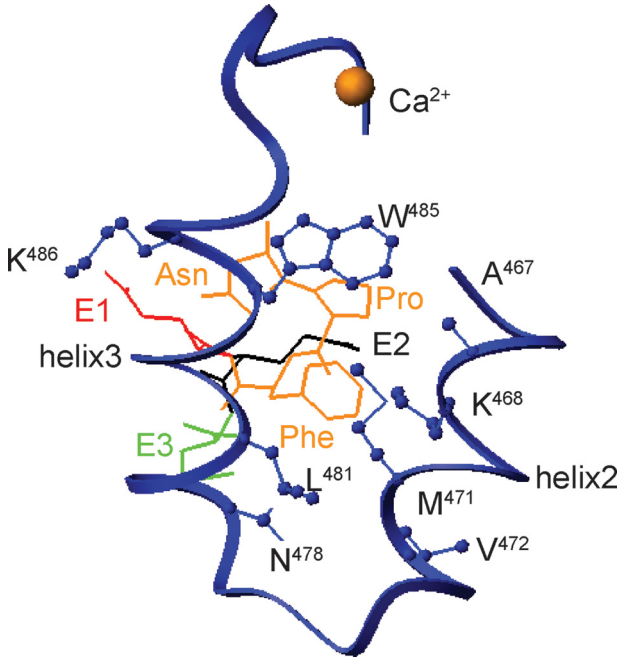

FIGURE 4. **Close-up view of the binding site between the EHD1 EH-domain and wild-type MICAL-L1 NPF_EEEEED peptide.** The EH-domain is colored *blue*, the NPF motif from the wild-type MICAL-L1 peptide is colored *orange*, and the acidic cluster E1, E2, and E3 from the wild-type MICAL-L1 peptide is colored *red*, *black*, and *green*, respectively. Residues involved in the direct interaction have been labeled.

helix 2 and 3 (Fig. 4). The Pro is localized in a hydrophobic core formed by Gly^{464}, Ala^{467}, Met^{471} and Trp^{485}. The complex is stabilized by a hydrogen bond between the Asn lateral chain and the carbonyl oxygen of Gly^{482}. We also observed a close proximity between the lateral chain of Lys^{486} with the first Glu (E1) and Lys^{468} with the second Glu (E2) leading to the formation of salt bridges between these residues which helped to stabilize the complex. Additionally, a few of the structures, including the lowest energy structure, have the third Glu (E3) positioned such that it could form a hydrogen bond with Asn^{478}.

Importance of the First Two Glutamic Acids in Fine Tuning the Binding Affinity for the C-terminal EH-domains—The structure of the EH-domain/wild-type MICAL-L1 peptide complex identified two salt bridges between EH-1 residues Lys^{486} and Lys^{468} and the peptide residues E1 and E2, respectively, which explains the significant decrease in affinity observed in the NMR experiment when they were substituted for Ala (Fig. 2). Because many of the known and potential EHD interaction proteins contain only two acidic residues following the NPF motif (see Table 1), NMR titrations were performed to determine how these proteins may compare with those containing three or more acid residues flanking the NPF motif, like following the first NPF motif of MICAL-L1. EH-1 was titrated with various concentrations of the Glu-to-Ala substituted peptides NPFEEAAAA, NPFEAAAAA, and NPFAEAAAA (Fig. 5). Compared with the wild-type MICAL-L1 peptide (57 μM ± 6) and the NPFEEEAAA peptide (54 μM ± 5) (Fig. 2), the binding affinity slightly decreases when E3 is substituted for Ala (NPFEEAAAA; 75 μM ± 9), but significantly decreases when the E2 or E1 is substituted for Ala. The binding affinity decreases for the NPFAEAAAA and NPFEAAAAA peptides to 187 μM ± 10 and 162 μM ± 11, respectively (Fig. 5). Interestingly, the observation that the NPFAEAAAA and NPFEAAAAA peptides have a reduced binding affinity similar to that of the NPFEEEEED peptide suggests that E1 and E2 are both important for optimal interactions. According to the solution structure of the complex, this is because of the interaction of E1 and E2 with EH-1 residues Lys^{486} and Lys^{468}, respectively.

To confirm that E1 and E2 are involved in forming a salt bridge with EH-1 Lys residues, NMR titrations were performed to look at the independence of binding at different salt concentrations, which would affect ionic interactions (Fig. 6, *A–C*). EH-1 was titrated with the wild-type MICAL-L1 peptide NPFEEEEED and the Glu-to-Ala substituted peptides NPFEEAAAA and NPFAAAEED. The buffer conditions were similar to those used to collect the titration data in Figs. 2 and 5 (20 mM deuterated Tris, 100 mM KCl, and 2 mM $CaCl_2$ at pH 7.0), except the KCl concentration was increased to 400 mM. The overall binding affinities for each of the peptides decreased in the presence of 400 mM KCl compared with 100 mM KCl (NPFEEEEED, 57 μM ± 6 to 185 μM ± 18; NPFEEAAAA, 75 μM ± 9 to 156 μM ± 11; NPFAAAEED 193 μM ± 13 to >1 mM); however, the binding affinity of the NPFEEAAAA peptide was similar to that of the wild-type peptide, not the NPFAAAEED peptide. This observation can be explained in that the NPFAAAEED peptide is able to form a hydrogen bond with EH-1 (Asn and Gly^{482}), whereas the NPFEEEEED and NPFEEAAAA peptides can form a hydrogen bond and salt bridges. In combination with the structural information (Figs. 3 and 4), the data suggest that E1 and E2 help stabilize the complex with EH-1 by forming a salt bridge with EH-1 residues Lys^{486} and Lys^{468}, respectively.

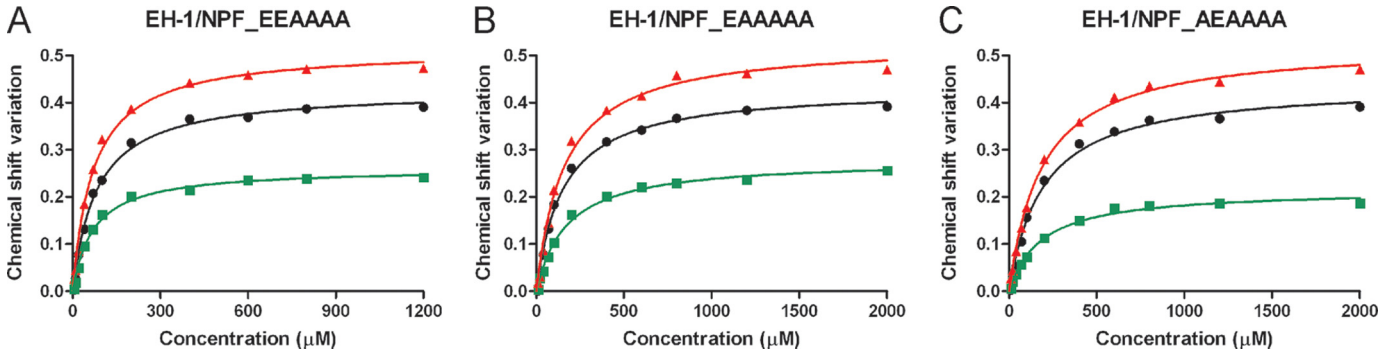

FIGURE 5. **Demonstration of the importance of the first two glutamic acids in fine tuning the binding affinity for the C-terminal EH-domains.** *A*, ^{15}N-HSQC of the EH-domain with different concentrations of MICAL-L1 Glu-to-Ala substituted peptides NPF_EEAAAA (*A*), NPF_EAAAAA (*B*), and NPF_AEAAAA (*C*). The same three EH-domain residues (Val^{472}, *red*; Gly^{482}, *black*; and Trp^{485}, *green*) were evaluated for each peptide. Each K_D was estimated by nonlinear best fitting the chemical shift variation (in parts/million) *versus* the concentration of peptide.

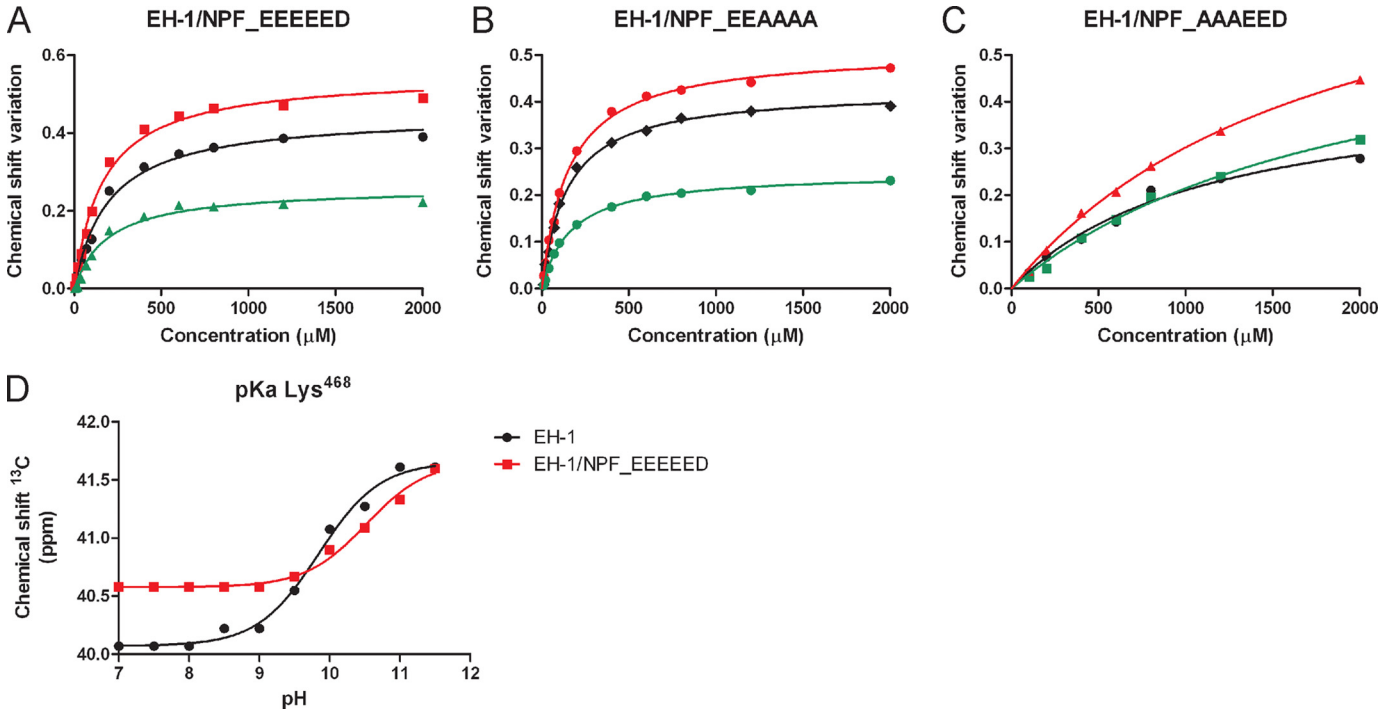

FIGURE 6. **Evidence that the first two glutamic acids form a salt bridge with EH-1 residues Lys^{486} and Lys^{468}.** *A–C*, ^{15}N-HSQC of the EH-domain with different concentrations of MICAL-L1 wild type peptide NPF_EEEEED and the Glu-to-Ala substituted peptides (*A*), NPF_EEAAAA (*B*), and NPF_AAAEED (*C*). The same three EH-domain residues (Val^{472}, *red*; Gly^{482}, *black*; and Trp^{485}, *green*) were evaluated for each peptide. Each K_D was estimated by nonlinear best fitting the chemical shift variation (in parts/million) *versus* the concentration of peptide. *D*, titration data for Lys^{468} at various pH values. The pH titration curves were fitted to the equation, $\delta = \delta_{min} + (\delta_{max} - \delta_{min})/(1 + 10^{pH - pK_a})$, where δ = chemical shift.

The possibility of a salt bridge between E2 and Lys^{468} was also confirmed by NMR titrations at different pH values, which would also affect ionic interactions (Fig. 6*D*). The ϵ carbon chemical shift from Lys^{468} was followed from pH 7.0 to 11.5. Unfortunately, the ϵ carbon from Lys^{486} was unable to be followed because of spectral overlap with the other 14 Lys residues. The ϵ carbon of Lys^{468} could be identified and followed because of shielding caused by the close proximity to the ring currents of Trp^{485}. The pK_a for EH-1 Lys^{468} alone was 9.85 ± 0.05, and in the presence of the wild-type MICAL-L1 peptide NPFEEEEED was 10.52 ± 0.08. This increase when in the complex is most likely caused by salt bridge formation between E2 and Lys^{468} (33).

Phage displayed screens for N-terminal EH-domain ligands, and NMR studies have identified that position +3 from the Asn contributes directly to the selectivity of NPF sequences by EH-domains (21, 22). Overduin and colleagues (21) observed a salt bridge between a Glu (from the human Eps15 s EH-domain and equivalent to the EHD1 residue Lys^{468}) and an Arg residue immediately following the NPF motif (from a synthetic peptide and equivalent to E1 in the MICAL-L1 peptide). Our data support the hypothesis that C-terminal EH-domains have evolved to use the exact opposite strategy in terms of charges. For example, C-terminal EH-domains have positively charged residues that prefer binding to NPF motifs flanked by negatively charged residues. In contrast, some N-terminal EH-domains selectively bind to NPF-containing proteins utilizing a negatively charged residue as a mechanism to ensure selectivity of binding to NPF motifs flanked by a positive residue. Therefore, we assessed how the binding affinity to EH-1 would be affected if E1 from the

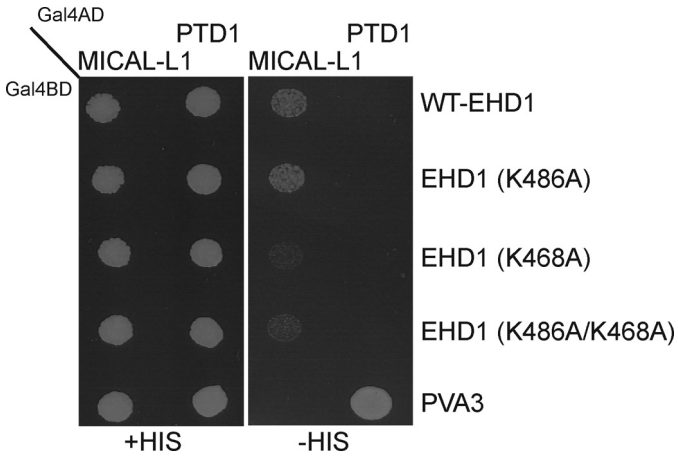

FIGURE 7. **Delineation of the EHD1 EH-domain residues that enhance affinity for MICAL-L1 by interaction with its NPF-flanking acidic cluster.** The *S. cerevisae* yeast strain AH109 was co-transformed with Gal4AD and Gal4BD fusion constructs containing MICAL-L1 with a mutated second NPF to APA and either wild-type (*WT*) or mutant EHD1 constructs (denoted in the *panel*). Co-transformants were assayed for their growth on nonselective (+*HIS*) and selective (−*HIS*) medium. PTD1 and PVA3 served as a positive control for protein-protein interaction.

MICAL-L1 peptide was replaced with an Arg residue. The EH-1 binding affinity for the NPFRAAAAA peptide was calculated to be 1,050 μM ± 48. This significant decrease compared with the NPFEAAAAA (162 μM ± 11) peptide suggests an electrostatic repulsion between Lys^{486} and the Arg residue (data not shown).

To provide further evidence in support of this selective mechanism for C-terminal EH-domain binding to acidic residue-flanked NPF motifs, we assessed the ability of EH-1 mutants to bind MICAL-L1 (ΔNPF2) (Fig. 7). As demonstrated, substitution of Lys^{468} for Ala caused an almost complete loss of binding in two-hybrid analysis, suggesting that the interaction of this residue with the second Glu following the MICAL-L1 NPF is indeed critical for the stability of this interaction. On the other hand, substitution of Lys^{486} with Ala did not have a discernible effect, and the double mutation (both Lys^{468} to Ala and Lys^{486} to Ala) displayed an effect that was similar to Lys^{468} alone. These data support a model in which a salt bridge between the second Glu flanking the NPF motif and Lys^{468} is required for an optimal interaction between the two proteins.

DISCUSSION

Despite the existence of hundreds of proteins that contain the tripeptide sequence motif NPF, the C-terminal EHD proteins interact with only a small subset of these, specifically, NPF-containing proteins that are implicated in the regulation of endocytic recycling events. Although one layer of specificity between EHD proteins and binding partners might arise as a result of "compartmentalization," the differential subcellular localization of these proteins within the cell, it was apparent that additional molecular mechanisms must be utilized to control this tight selectivity.

The solution structure of the EHD1 EH-domain (EH-1) (19) and our observations that the other EHD paralogs have EH-domains with highly positively charged surface areas (1) originally led us to hypothesize that C-terminal EH-domains might selectively recognize the more acidic DPF motifs (as opposed to NPF motifs). However, because no DPF-containing interaction partners for EHD1 have been discovered and because our NMR data indicate that DPF motifs bind to EH-1 with lower affinity (30), we began to examine alternative explanations as to why C-terminal EH-domains contain such a positively charged surface. An important clue came from the empiric observation that most NPF motifs that bind to EH-1 contain acidic residues flanking the NPF (see Table 1) (for review, see Ref. 1). In addition, we found that a number of NPF-containing proteins that bind to N-terminal EH-domains show little or no binding to C-terminal EH-domains (30). Cumulatively, this led us to propose that the selective binding of C-terminal EH-domains with a specific subset of NPF-containing proteins might result from a mechanism that allows the formation of additional bonds that contribute to the affinity between the positively charged C-terminal EH-domain surface and the acidic residues flanking the NPF motif.

The selectivity of various N-terminal EH-domains for NPF peptides was addressed by the study of Paoluzi *et al.* (22), who used phage display experiments to analyze the preference of various mammalian and yeast EH-domains for NPF peptides. It is of great interest that none of the six EH-domains derived from the mammalian Eps15 and Eps15R showed any preference for binding to peptides that contained acidic clusters following the NPF. Moreover, a considerable number of these EH-domains did show preference for binding to an NPF motif followed by the positively charged Arg residue (22). In contrast, we have determined that an Arg residue flanking the NPF motif actually repulses EH-1 binding, and such peptides display dramatically reduced affinity for EH-1. In agreement with these findings, we searched the data banks for proteins containing the sequence NPFR and identified >40 human proteins with additional isoforms, none of which is known to interact with EHDs (partial list displayed in Table 1). On the other hand, at least one of these proteins is known to interact with N-terminal EH-domain-containing proteins (SYNJ1; synaptojanin1), and several of these proteins have known roles in internalization events (SYNJ1, TBD2A).

We have now elucidated a molecular mechanism that underlies the selective interactions of C-terminal EH-domains with a specific subset of NPF-containing proteins involved in the regulation of endocytic recycling. Based on the solution structure of the EH-1 in complex with the MICAL-L1 NPF peptide (NPFEEEEED), it is clear that the flanking acidic residues are in close proximity of the positively charged residues within the EH-domain. Although the NPF motif formed the classic type I β-turn for NPF motif when bound to an EH-domain, we also observed that the side chain of Lys^{486} with the first Glu (E1), Lys^{468} with the second Glu (E2), and possibly Asn^{478} with the third Glu (E3) lie in a position to form a salt bridge. The formation of these salt bridges is consistent with our NMR data, demonstrating a graded decrease in binding affinity when each of these three Glu residues was substituted with Ala. The NMR data also suggests that acidic residues at positions E4, E5, and D6 do not directly influence the contact with EH-1 to stabilize the complex because the binding affinities are similar between the NPFEEEEED and NPFEEEAAA peptides.

Our data support a molecular mechanism by which NPF-containing proteins involved in the regulation of endocytic recycling events have co-evolved along with C-terminal EH-domains to arrive at higher affinity interactions resulting from salt bridges between acidic residues flanking the NPF with positively charged residues on the C-terminal EH-domain surface. Interestingly, by searching the protein data banks we have identified a series of proteins with NPF motifs flanked by such acidic clusters (Table 1); although these have yet to be identified as EHD interactors, several of these proteins are involved in endocytic events, including EXOC8 (34), AAK1 (35), and LYST (25), and we predict that they are likely to interact with C-terminal EHDs.

REFERENCES

1. Grant, B. D., and Caplan, S. (2008) *Traffic* **9,** 2043–2052
2. Daumke, O., Lundmark, R., Vallis, Y., Martens, S., Butler, P. J., and McMahon, H. T. (2007) *Nature* **449,** 923–927
3. Lee, D. W., Zhao, X., Scarselletta, S., Schweinsberg, P. J., Eisenberg, E., Grant, B. D., and Greene, L. E. (2005) *J. Biol. Chem.* **280,** 17213–17220
4. Naslavsky, N., Rahajeng, J., Sharma, M., Joviæ, M., and Caplan, S. (2006) *Mol. Biol. Cell* **17,** 163–177
5. Miliaras, N. B., and Wendland, B. (2004) *Cell Biochem. Biophys* **41,** 295–318
6. Naslavsky, N., and Caplan, S. (2005) *J. Cell Sci.* **118,** 4093–4101
7. Grant, B., Zhang, Y., Paupard, M. C., Lin, S. X., Hall, D. H., and Hirsh, D. (2001) *Nat. Cell Biol.* **3,** 573–579
8. Lin, S. X., Grant, B., Hirsh, D., and Maxfield, F. R. (2001) *Nat. Cell Biol.* **3,** 567–572
9. Caplan, S., Naslavsky, N., Hartnell, L. M., Lodge, R., Polishchuk, R. S., Donaldson, J. G., and Bonifacino, J. S. (2002) *EMBO J.* **21,** 2557–2567
10. Rapaport, D., Auerbach, W., Naslavsky, N., Pasmanik-Chor, M., Galperin, E., Fein, A., Caplan, S., Joyner, A. L., and Horowitz, M. (2006) *Traffic* **7,** 52–60
11. Naslavsky, N., McKenzie, J., Altan-Bonnet, N., Sheff, D., and Caplan, S. (2009) *J. Cell Sci.* **122,** 389–400
12. Gokool, S., Tattersall, D., and Seaman, M. N. (2007) *Traffic* **8,** 1873–1886
13. George, M., Ying, G., Rainey, M. A., Solomon, A., Parikh, P. T., Gao, Q., Band, V., and Band, H. (2007) *BMC Cell Biol.* **8,** 3
14. Sharma, M., Naslavsky, N., and Caplan, S. (2008) *Traffic* **9,** 995–1018
15. Guilherme, A., Soriano, N. A., Bose, S., Holik, J., Bose, A., Pomerleau, D. P., Furcinitti, P., Leszyk, J., Corvera, S., and Czech, M. P. (2004) *J. Biol. Chem.* **279,** 10593–10605
16. Park, S. Y., Ha, B. G., Choi, G. H., Ryu, J., Kim, B., Jung, C. Y., and Lee, W. (2004) *Biochemistry* **43,** 7552–7562
17. Fazioli, F., Minichiello, L., Matoskova, B., Wong, W. T., and Di Fiore, P. P. (1993) *Mol. Cell. Biol.* **13,** 5814–5828
18. Wong, W. T., Schumacher, C., Salcini, A. E., Romano, A., Castagnino, P., Pelicci, P. G., and Di Fiore, P. P. (1995) *Proc. Natl. Acad. Sci. U.S.A.* **92,** 9530–9534
19. Kieken, F., Jović, M., Naslavsky, N., Caplan, S., and Sorgen, P. L. (2007) *J. Biomol. NMR* **39,** 323–329
20. de Beer, T., Carter, R. E., Lobel-Rice, K. E., Sorkin, A., and Overduin, M. (1998) *Science* **281,** 1357–1360
21. de Beer, T., Hoofnagle, A. N., Enmon, J. L., Bowers, R. C., Yamabhai, M., Kay, B. K., and Overduin, M. (2000) *Nat. Struct. Biol.* **7,** 1018–1022
22. Paoluzi, S., Castagnoli, L., Lauro, I., Salcini, A. E., Coda, L., Fre', S., Confalonieri, S., Pelicci, P. G., Di Fiore, P. P., and Cesareni, G. (1998) *EMBO J.* **17,** 6541–6550
23. Salcini, A. E., Confalonieri, S., Doria, M., Santolini, E., Tassi, E., Minenkova, O., Cesareni, G., Pelicci, P. G., and Di Fiore, P. P. (1997) *Genes Dev.* **11,** 2239–2249
24. Confalonieri, S., and Di Fiore, P. P. (2002) *FEBS Lett.* **513,** 24–29
25. Barbosa, M. D., Nguyen, Q. A., Tchernev, V. T., Ashley, J. A., Detter, J. C., Blaydes, S. M., Brandt, S. J., Chotai, D., Hodgman, C., Solari, R. C., Lovett, M., and Kingsmore, S. F. (1996) *Nature* **382,** 262–265
26. Linge, J. P., O'Donoghue, S. I., and Nilges, M. (2001) *Methods Enzymol.* **339,** 71–90
27. Laskowski, R. A., Rullmannn, J. A., MacArthur, M. W., Kaptein, R., and Thornton, J. M. (1996) *J. Biomol. NMR* **8,** 477–486
28. Koradi, R., Billeter, M., and Wuthrich, K. (1996) *J. Mol. Graph.* **14, 51–55,** 29–32
29. Naslavsky, N., Boehm, M., Backlund, P. S., Jr., and Caplan, S. (2004) *Mol. Biol. Cell* **15,** 2410–2422
30. Kieken, F., Jović, M., Tonelli, M., Naslavsky, N., Caplan, S., and Sorgen, P. L. (2009) *Protein Sci.* **18,** 2471–2479
31. Sharma, M., Giridharan, S. S., Rahajeng, J., Naslavsky, N., and Caplan, S. (2009) *Mol. Biol. Cell* **20,** 5181–5194
32. Nishimura, N., and Sasaki, T. (2008) *J. Med. Invest.* **55,** 9–16
33. Gao, G., DeRose, E. F., Kirby, T. W., and London, R. E. (2006) *Biochemistry* **45,** 1785–1794
34. Zhang, X., Zajac, A., Zhang, J., Wang, P., Li, M., Murray, J., TerBush, D., and Guo, W. (2005) *J. Biol. Chem.* **280,** 20356–20364
35. Conner, S. D., and Schmid, S. L. (2002) *J. Cell Biol.* **156,** 921–929